Hemispherical Lens Based Imaging Receiver for MIMO Optical Wireless Communications

Thomas Q. Wang, Y. Ahmet Sekercioglu and Jean Armstrong
Department of Electrical and Computer Systems Engineering
Monash University
Melbourne, Australia
{Tom.Wang, Ahmet.Sekercioglu, Jean.Armstrong}@monash.edu

***Abstract*—White lighting LED based systems are emerging as an important form of high data rate communications, especially for indoor applications. Two limitations of existing systems are the small field of view of typical receivers and the poor performance of optical wireless MIMO due to lack of spatial diversity. In this paper we describe a novel design which overcomes these problems by using a hemispherical lens in the receiver. We show that the new system has a wide field of view and also provides significant spatial diversity for typical MIMO visible light scenarios. Numerical results are provided for a range of LED transmitters with different half power semi-angles. Our analysis shows that systems can be designed with adequate channel gain for angles of incidence as large as 70 degrees. The optical power density is also calculated to show the received optical power distributions for the case of four LED transmitters. The results indicate that the images of the LEDs are clearly separated. This reduces the channel correlations between individual transmitters and receivers and thus promises a significant diversity order for MIMO optical wireless systems.**

Keywords- optical wireless communications, MIMO, imaging receiver, hemispherical lens, diversity

I. INTRODUCTION

Due to their energy efficiency, white light emitting diodes (LEDs) are rapidly replacing conventional fluorescent and incandescent lights. Although designed primarily for lighting, unlike conventional light sources, white LEDs can be modulated at frequencies up to 20 MHz [1] and as a result can form the basis of a range of novel data communication systems [2]-[8]. However, two major limitations, the small field of view (FOV) of typical receivers, and the lack of diversity in MIMO systems need to be overcome first to realize the potential of white LEDs [3][6].

In the context of optical wireless, receivers can be classified as 'imaging' or 'non-imaging' [3][8]. Recent research has shown that the advantage of MIMO in non-imaging optical systems is relatively limited and that imaging receivers potentially offer better performance [3]. In the research literature, two forms of MIMO imaging systems have been described [4][5][8]-[10]. In [4] a number of directional receivers are used. Although this arrangement provides diversity and therefore increases data rates, it is bulky and not easily scalable. The second form is based on standard camera technology [5][9][10]. Standard cameras are designed to have a FOV that matches the human eye, and to produce focused images [11]. This is in contrast to MIMO optical wireless, where, in many cases, a much wider FOV is desirable, so that the probability of maintaining a LOS is maximized. Lenses with wide FOV produce distorted images. This is a limitation for photography and image processing applications, but may not be a problem for MIMO optical wireless communications.

The most viable modulation and demodulation technology for optical wireless is intensity modulation and direct detection (IM/DD). In IM/DD systems, the intensity of the light carries the information. Thus, all the transmitted information-carrying signals have nonnegative values. Also, in IM/DD optical systems, the channel gain is given by the ratio of the received optical power to the transmitted optical power [6]. Therefore, unlike the complex gain of an RF channel, the channel gain of optical wireless is always real and positive. In the MIMO optical wireless context, multiple LEDs work as transmitters, emitting modulated signals and the photodetectors detect the intensity of the received signals. Consequently, as in MIMO RF channels, the optical wireless channels between the LEDs and the photodetectors can also be represented by a channel matrix. However, unlike RF, the channel matrix for optical wireless is a real matrix with its elements denoting the power gains of all the LED-photodetector pairs.

Light propagating from each LED to a photodetector is generally made up of two components, the LOS component which transmits from the LED to the receiver directly and the diffuse component which propagates via reflections. Previous studies have shown that the LOS component is usually much stronger than the diffuse component [3][12]. In this paper, we consider only the LOS component and leave analysis of multi-path transmission for a future study.

In this paper, we analyze a novel receiver configuration using a hemispherical lens. Compared with other optical MIMO systems, the new configuration can (i) receive the light signal from a large angle of incidence, which provides a wide FOV for the receiver and (ii) separate the signals from different LEDs effectively. This reduces the correlations between the elements of the channel matrix. The larger FOV enables LOS communications in more cases, and thus improves the SNR at the photodetector. The low correlations between the elements of the channel matrix promise spatial diversity for MIMO systems.

II. System Description and Analysis

Consider the imaging system shown in Fig. 1. N_t white LED ceiling lights illuminate the room and transmit data. In this study, we treat each light source as a single LED. In practice, a LED light fitting may be made up of a cluster of individual LEDs. The receiver is composed of two parts - a hemispherical lens used to refract the emitted light, and an array of N_r photodetectors.

The photodetectors can be in the form of the individual pixels of a camera sensor, in which case the array may have a very large number of elements, or alternatively the array can consist of a small number of individual photodetectors. Denote the $N_r \times N_t$ channel matrix between the LEDs and the receiver by $\mathbf{H}$. Then the element $\mathbf{H}(i, j)$ is the channel gain between the ith photodetector and the jth LED.

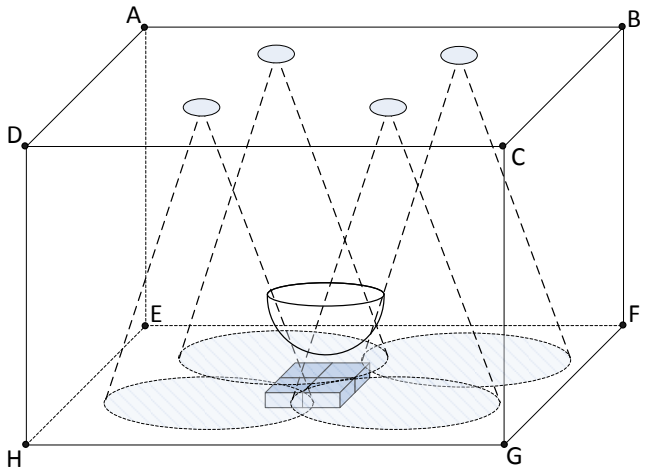

Figure 1. Schematic of the imaging system configuration for MIMO optical wireless communication. The transmitters are on the ceiling and pointing down, the photodetectors are arranged on the floor pointing to the ceiling.

Fig. 2 shows the geometrical model of the new receiver in a spherical coordinate system. A LED is placed at point $S:(l\sin\varphi\cos\theta, l\sin\varphi\sin\theta, l\cos\varphi)$, directed downwards and emits un-polarized white light. The origin of the coordinate system is at the center of the flat surface of the lens which is on the *xOy* plane. Thus, by definition of the spherical coordinate system, l, φ and θ denote the distance to the center of the flat surface of the lens, the angle between *SO* and the positive *z* axis, and the angle between *S′O* and the positive *x* axis, respectively. We assume the LED is at a distance much greater than R, the radius of the lens (i.e. $l >> R$). Thus, we can assume that light rays coming from the LED arrive at the flat surface of the lens with approximately the same angle of incidence, φ, after travelling the same distance, l (i.e. *SO* can be regarded as (approximately) parallel to *SA* in Fig. 2). The photodetector array is located on the plane $z = f, f < -R$. Suppose the LED emits an axially symmetric radiation pattern, then the irradiance on the flat surface of the lens can be expressed as

$$I_s(l,\phi) = P_t R_o(\phi)/l^2, \tag{1}$$

where ϕ denotes the angle of emission relative to the optical axis of the LED [6]. P_t is the transmit power and $R_o(\phi)$ is the generalized Lambertian radiation pattern [6][13] which can be expressed as

$$R_o(\phi) = \frac{(m+1)}{2\pi}\cos^m\phi$$

The order m is related to $\Phi_{1/2}$, which is the transmitter semi-angle at half power, by $m = -\ln 2/\ln(\cos\Phi_{1/2})$.

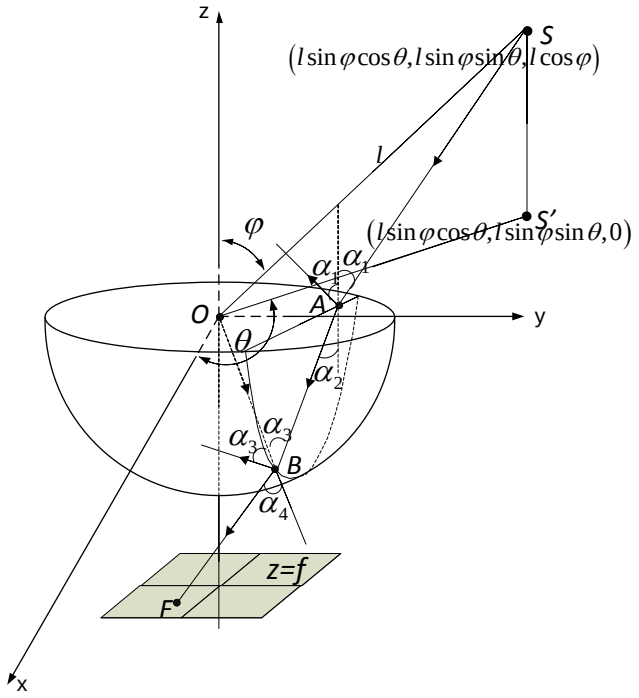

Figure 2. Geometrical model of the hemispherical lens and photodetector

When the light rays arrive at the flat surface of the lens at a given point, for example $A:(r\cos\beta, r\sin\beta)$, part of the power is lost due to the reflected rays. The proportion of the light which is reflected depends on the angle of incidence, $\alpha_1 = \varphi$, the refractive indexes n_1 (for the air) and n_2 (for the lens), and is given by the Fresnel equations [14]

$$R_p(\alpha_1,\alpha_2) = \frac{n_1\cos\alpha_2 - n_2\cos\alpha_1}{n_1\cos\alpha_2 + n_2\cos\alpha_1} \tag{2}$$

and

$$R_s(\alpha_1,\alpha_2) = \frac{n_1\cos\alpha_1 - n_2\cos\alpha_2}{n_1\cos\alpha_1 + n_2\cos\alpha_2} \tag{3}$$

where R_p and R_s denote the reflection coefficients of *p*-polarized and *s*-polarized light, respectively and α_2 is the angle of refraction and which is related to α_1 by Snell's law.

$$n_1 \sin\alpha_1 = n_2 \sin\alpha_2 \tag{4}$$

For unpolarized light, the power transmission coefficient of the flat surface is given by

$$T_{\text{air-lens}}(\alpha_1) = 1 - \frac{1}{2}\left(R_{\text{s}}^2(\alpha_1,\alpha_2) + R_{\text{p}}^2(\alpha_1,\alpha_2)\right) \tag{5}$$

The refracted ray then travels to point B on the curved surface of the lens. We assume that the power loss inside the lens is negligibly small. Suppose the angle the ray makes with the normal of the curved surface at point B is α_3, i.e. the angle of incidence is α_3. Then the refracted angle α_4 is related to α_3 by Snell's law (4). Note that α_3 and α_4 depend on the coordinates of the point A and the coordinates of the LED. Therefore, the power transmission coefficient of the curved surface is a function of S, r and β. Also note that total internal reflection occurs when α_3 is beyond the critical angle, $\arcsin(n_1/n_2)$. In this case, there is no light refracted out of the lens. Although part of these light rays may pass through the lens and hit the photodetector after multiple internal reflections within the lens, the power of these rays is attenuated severely by the reflections, (see (2),(3) and (5)). Therefore, we assume they are lost.

When α_3 is smaller than the critical angle, part of the power of the rays is refracted out of the lens and finally reaches the photodetector array generating the photo-current for detection. The amount of the power that is refracted out of the lens can be found by exchanging n_1 and n_2 in (2) and (3) and then substituting α_1 and α_2 in (5) by α_3 and α_4, respectively, to give

$$T_{\text{lens-air}}(\alpha_3,\alpha_4) = 1 - \frac{1}{2}\left(R_{\text{s}}^2(\alpha_3,\alpha_4) + R_{\text{p}}^2(\alpha_3,\alpha_4)\right) \tag{6}$$

As in [3] and [15], the channel gain is defined as the ratio of the power received at the photodetector P_o and the power transmitted by the LED P_t, i.e.

$$T = P_o / P_t \tag{7}$$

By integrating over all the points for which the rays reach the photodetector, the channel gain can be found. For the case where there is a single photodetector large enough to collect all of the light which passes through the lens

$$T = \frac{P_o}{P_t} = \frac{(m+1)\cos^m\phi\cos\varphi T_{\text{air-lens}}(\alpha_1)}{2\pi l^2} \times \iint_{\alpha_3 < \arcsin(n_1/n_2)} T_{\text{lens-air}}(\alpha_3,\alpha_4)\, r dr d\beta \tag{8}$$

We plot the channel gain given by (8) with varying parameter settings using a LED with semi-angle $\Phi_{1/2} = 15^o$ and a lens (1.5 index of refraction) with 5mm diameter. In Figs. 3 and 4, the channel gain versus the distance l, and channel gain versus the angle of incidence α_1 graphs are presented respectively. As the figures show, the channel gain drops with increasing distance to the LED, and it also decreases with increasing angle of incidence.

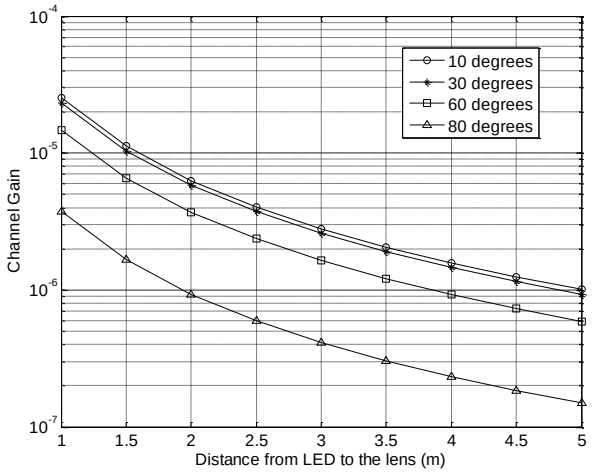

Figure 3. Channel gains versus the distance from the LED to the imaging receiver with varying angle of incidence

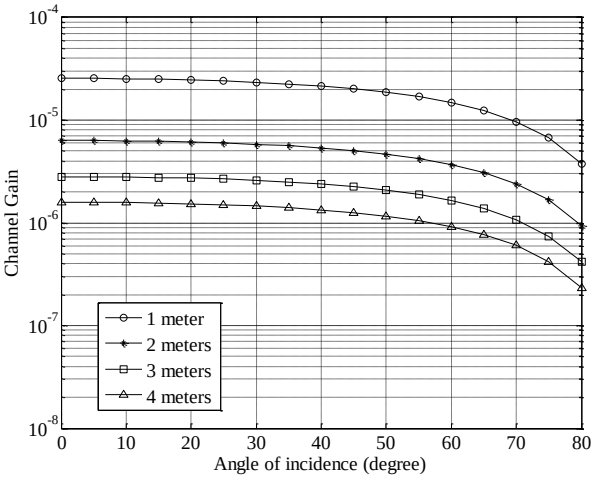

Figure 4. Channel gains versus the angle of incidence with varying distances from the LED to the imaging receiver

III. Simulation Results

Here, we present results for a typical $5m \times 5m \times 2.5m$ room with four transmitters on the ceiling (Fig. 1). Since the transmitters point down and receivers point up, we have $\alpha_1 = \varphi = \phi$. Note that, the distance l changes when we increase or decrease the angle of incidence. The diameter of the hemispherical lens is 5 mm and its index of refraction is 1.5. The lens is placed above the photodetector array at a distance of 5 mm from the vertex of the curved surface to the photodetector. Consequently, the distance from the flat surface of the lens to the ceiling is approximately 2.5 *m*. Therefore, we can calculate that the angle of incidence, α_1, achieves its

maximum at 70.5 degrees when a LED is placed at one of the corners of ceiling and the photodetector at the furthest corner on the floor.

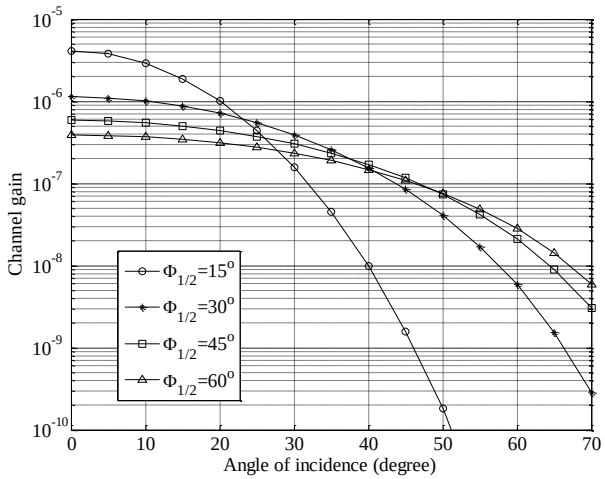

Figure 5. Channel gains versus the angle of incidence for Lambertian emiiters with varying half power semi-angles

First, we study a single input-single output (SISO) system. The single photodetector is assumed to be large enough to collect all the light passing through the lens. In Fig. 5, channel gains versus the angle of incidence are plotted for various generalized Lambertian LEDs. The half power semi-angles considered are $\Phi_{1/2} = 15^o$, 30^o , 45^o and 60^o respectively. Without loss of generality, we normalize the transmitted power to unity. Thus, the received power on the photodetector indicates the channel gain. As shown in Fig. 5, all the channel gains decrease dramatically with the angle of incidence. This is because (i) the reflection coefficient of the lens increases with the angle of incidence, and (ii) the effective area of the flat surface of the lens changes in proportion to $\cos\alpha_1$. Since, the LED with higher directionality transmits more power in the direction of its axis, the LEDs with smaller $\Phi_{1/2}$ (15^o and 30^o) provide larger channel gains than the ones with lower directionality when the angle of incidence is small, say less than 23 degrees in this figure. However, as the angle of incidence increases, less power reaches the lens for the emitter with small $\Phi_{1/2}$ than for the ones with large $\Phi_{1/2}$ (lower directionality). As a result, the channel gain of the LEDs with high directionality falls much more rapidly than for the other LEDs. Fig. 5 also shows that the LED with 60 degrees semi-angle provides the highest channel gain for angles of incidence greater than 45 degrees. In this case, the imaging system can provide a very wide FOV.

Next, we study a MIMO system with four LEDs. Geometrically, we put four LEDs with 60^o of semi-angle at:
$T_x^{(1)} : \left(l = 2.5/\cos\varphi, \varphi = 30^o, \theta = 45^o\right)$,
$T_x^{(2)} : \left(l = 2.5/\cos\varphi, \varphi = 30^o, \theta = 135^o\right)$,
$T_x^{(3)} : \left(l = 2.5/\cos\varphi, \varphi = 30^o, \theta = 225^o\right)$,
and
$T_x^{(4)} : \left(l = 2.5/\cos\varphi, \varphi = 30^o, \theta = 315^o\right)$ in the spherical coordinate system in Fig. 2. We plot the optical power density generated at the photodetector array in Fig. 6. As shown in the figure, the signals from different LEDs are clearly separated, with the majority of the power from a given LED being received in a single quadrant. To demonstrate the diversity that can be achieved we consider the case where there are four photodetectors, and each photodetector collects all of the light in one of the quadrants of Fig. 6. The channel matrix for this configuration was calculated by integrating the received power density due to each LED over each quadrant to give

$$\mathbf{H} = \begin{bmatrix} 0.009 & 0.151 & 1.124 & 0.151 \\ 0.152 & 0.01 & 0.157 & 1.13 \\ 1.136 & 0.158 & 0.011 & 0.158 \\ 0.152 & 1.13 & 0.157 & 0.01 \end{bmatrix} \times 10^{-6} \qquad (9)$$

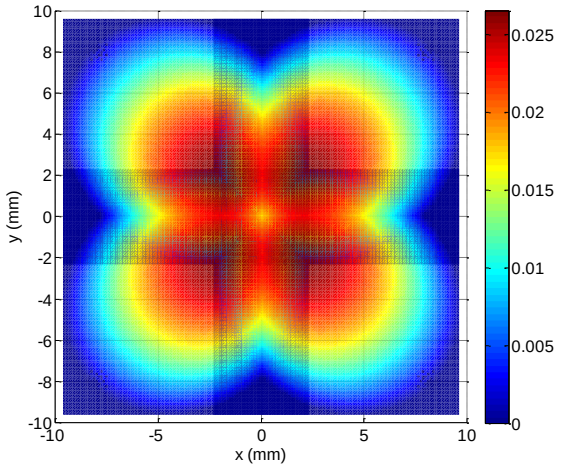

Figure 6. Power density on the photodetectors with 30 degrees of the angle of incidence

Note that in each row or column, there is one element which is much larger than the others. This indicates that (i) for a given photodetector, almost all the power it receives comes from a single LED and (ii) for a given LED, almost all of the power that passes through the lens is received by a single photodetector. Therefore, there is little correlation between the rows (columns) of the channel matrix when the new system is used. The resulting channel matrix is invertible even though there is interchannel interference. Thus, the transmitted data can be decoded by using the method described in [3]. Consequently, the new technique can form the basis of MIMO systems with high spatial diversity. This is in contrast to a non-imaging receiver where its photodetector does not use a lens [3]. Since the size of the photodetector array is usually much smaller than the distance l , the rays from any given LED can be regarded as parallel as they reach the photodetectors. The distance from each photodetector to a LED varies very little. From (1), we can see that the irradiance each photodetector receives from a given LED would be almost identical. This results in a channel matrix in which the columns are highly

correlated. In the worst case, the rank of the matrix may decrease to 1, which leads very high bit error rate (BER) as in [3].

Finally, we consider the effect of placing the LEDs further apart so that the angle of incidence for each increases. Fig. 7 shows the result for $\varphi = 60^o$, and as can be seen from the figure, the images of the four LEDs are now completely distinct. In this situation, the columns of the channel matrix are orthogonal. Thus, the normalized form of the channel matrix can be expressed as

$$\mathbf{H} = \begin{bmatrix} 0 & 0 & 1 & 0 \\ 0 & 0 & 0 & 1 \\ 1 & 0 & 0 & 0 \\ 0 & 1 & 0 & 0 \end{bmatrix} \tag{10}$$

Eq. (10) and Fig. 7 show that each photodetector can receive signal from only one LED. Thus, there is no interchannel interference between channels, which leads to higher SNR at each photodetector. Note that the orthogonal structure of the channel matrix also reduces the decoding complexity. Since each photodetector receives the signal only from its corresponding LED, the decoding can be performed as in a SISO system without interference.

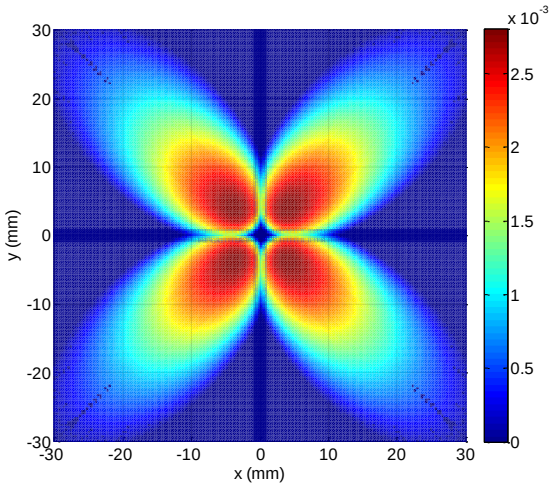

Figure 7. Power density on the photodetectors with 60 degrees of the angle of incidence

IV. CONCLUSION

This paper presents a novel imaging MIMO optical wireless system which uses a hemispherical lens in the receiver. The new system has both wide FOV and significant spatial diversity. Results are presented for a number of typical indoor optical wireless communications scenarios. The dependence of channel gain on angle of incidence is calculated for LEDs with a range of half angles. The channel gain of LEDs with small half angles is greater for small angles of incidence, but falls off quickly as the angle of incidence increases. The received optical power density is also plotted for a scenario with four symmetrically placed LED transmitters. The channel matrix for this 4×4 MIMO system is calculated showing that the new system can provide significant spatial diversity.

REFERENCES

[1] J. R. Barry, J. M. Kahn, E. A. Lee and D. G. Messerschmitt, "High-speed nondirective optical communication for wireless networks," *IEEE Network Magazine*, vol. 5, no. 6, pp. 44-54, Nov. 1991.

[2] M. Kavehrad and S. Jivkova, "Indoor broadband optical wireless communications: optical subsystems designs and their impact on channel characteristics," *IEEE Wireless Communications*, vol.10, no.2, pp. 30-35, Apr. 2003.

[3] L. Zeng, D. C. O'Brien, H. L. Minh, G. E. Faulkner, K. Lee, D. Jung, Y. Oh and E. T. Won, "High data rate multiple input multiple output (MIMO) optical wireless communications using white led lighting," *IEEE Journal on Selected Areas in Communications*, vol. 27, no. 9, pp.1654-1662, Dec. 2009.

[4] K. D. Dambul, D.C. O'Brien and G.. Faulkner, "Indoor Optical Wireless MIMO System With an Imaging Receiver," *IEEE Photonics Technology Letters*, vol. 23, no. 2, pp. 97-99, Jan. 2011.

[5] S. Hranilovic and F.R. Kschischang, "A pixelated MIMO wireless optical communication system," *IEEE Journal of Selected Topics in Quantum Electronics*, vol. 12, no. 4, pp. 859-874, July/Aug. 2006.

[6] J. M. Kahn and J. R. Barry, "Wireless Infrared Communications," *Proceedings of the IEEE*, vol. 85, no. 2, pp. 265-298, Feb, 1997.

[7] J.M. Kahn, R. You, P. Djahani, A. G. Weisbin, B. K. Teik and A. Tang, "Imaging diversity receivers for high-speed infrared wireless communication," *IEEE Communications Magazine*, vol. 36, no. 12, pp. 88-94, Dec. 1998.

[8] D. C. O'Brien, "Multi-Input Multi-Output (MIMO) indoor optical wireless communications," *Signals, Systems and Computers, 2009 Conference Record of the Forty-Third Asilomar Conference on*, pp. 1636 – 1639, Nov. 2009.

[9] S. D. Perli, N. Ahmed, and D. Katabi, "PixNet: Interference-Free Wireless Links Using LCD-Camera pairs," *In Proceedings of MOBICOM'2010*, Chicago, pp.137-148, 2010..

[10] W. Yuan, K. Dana, M. Varga, A. Ashok, M. Gruteser and N. Mandayam, "Computer vision methods for visual MIMO optical system," *in Computer Vision and Pattern Recognition Workshops (CVPRW), 2011 IEEE Computer Society Conference on*, pp. 37-43, 2011.

[11] M. J. Langford, A. Fox, and R.S. Smith, "Langford's basic photography the guide for serious photographers 9th Edition," Focal Press.

[12] L. Zeng, D. C. O'Brien, H. Le-Minh, L. Kyungwoo, J. Daekwang, and O. Yunje, "Improvement of Date Rate by using Equalization in an Indoor Visible Light Communication System," *in Proc. IEEE ICCSC*, pp. 678-682, 2008.

[13] F. R. Gfeller and U. H. Bapst, "Wireless in-house data communication via diffuse infrared radiation," *Proc. IEEE*, vol. 67, pp. 1474–1486, Nov. 1979.

[14] K. D. Möller, "Optics," University Science Books, Mill Valley, California.

[15] J. R. Barry, J. M. Kahn, W. J. Krause, E. A. Lee, and D. G. Messerschmitt, "Simulation of multipath impulse response for wireless optical channels," *IEEE J. Select. Areas in Commun.*, vol. 11, no. 3, pp. 367–379, Apr. 1993.